Dynamic Behavior of Core-material Penetration in Multi-Cavity Co-Injection Molding

Jackie Yang[1], Chao-Tsai (CT) Huang[1], Hsien-Sen Chiu[1], Jimmy C.Chien[1], and *Anthony Wen-Hsien Yang [2]*
1. *CoreTech System (Moldex3D) Co., Ltd., Hsinchu, Taiwan*
2. *Moldex3D North America, Inc, USA*

Abstract

Co-Injection Molding and multi-cavity molding are very common processes for plastic manufacturing. These two systems are sometimes combined and applied to forks structure products. The core penetration and flow balance control problems are very difficult to manage. The inside mechanism of co-injection multi-cavity system is not fully figured out yet. In this study, we have focused on the dynamic behavior of core-material penetration in a co-injection multi-cavity molding. The dynamic behavior of core penetration is very sensitive to injection speed and skin/core ratio. The largest core penetration has been shown to change dramatically from one runner to the other. In addition, the core penetration behavior will display imbalance at the end of filling. The more core ratio it is, the longer core penetration flows through runner to cavity. However, due to the multi-cavity geometrical structure, the balance of the core penetration for multi-cavity is still challenging. Finally, the simulation is validated with the literature result [9]. These results show both simulation and experiments are in a good agreement in trend.

Introduction

Co-injection multi-component molding has been developed and applied into industries for many years. Basically, varies skin/core material combinations, are commonly used in daily accessories like automotive components and structural reinforcement product. Such as soft in the skin/hard in the core, fresh skin/regrind core, raw skin/reinforcement core [1-2]. Some well-known advantages of co-injection is to reduce cost, reuse material, and upgrade production efficiency. Besides, strength of structural reinforcement product is correlated to skin/core material distribution, therefore the control of internal material distribution is important. The correlation between internal material distributions, process condition, and material property are established in our previous research [3]. The cavity-filling ratio of skin material determines the break-through location. Material viscosity and filling rate affect uniformity of core material distribution. However, there are too many combinations of designs, materials, core/skin ratio, and process condition. It is challenging to have suitable control of co-injection.

On the other hand, imbalance filling behavior is very common in multi-cavity molding. Even for the geometrically balanced runner system of multi-cavity.

When the imbalanced filling occurred between different cavities, inter-cavity variation and intra-cavity variation will happen. For non-geometrically balanced runner system of multi-cavity, the flow imbalance become more complicated [4-8].

Furthermore, co-injection with multi-cavity molding system which is applied broadly in some forks structure products as shown in Figure 1 here and Figure 1 of Reference 9 [9-10]. The inside mechanism for the combination of co-injection and multi-cavity is not fully understood yet. In this study, we will focus on dynamic behavior of core-material penetration in a co-injection multi-cavity molding. We particularly investigate the core-material penetration features under different skin/core ratio, different injection speed, and melting temperatures. Also, the experimental validation has been performed based on Yokoi et al. studied [9].

Numerical Simulation

The polymer melt is assumed as General Newtonian Fluid (GNF). Hence the non-isothermal 3D flow motion can be mathematically described by the following:

$$\frac{\partial \rho}{\partial t} + \nabla \cdot \rho \mathbf{u} = 0 \tag{1}$$

$$\frac{\partial}{\partial t}(\rho \mathbf{u}) + \nabla \cdot (\rho \mathbf{u}\mathbf{u} - \boldsymbol{\sigma}) = \rho \mathbf{g} \tag{2}$$

$$\boldsymbol{\sigma} = -p\mathbf{I} + \eta (\nabla \mathbf{u} + \nabla \mathbf{u}^T) \tag{3}$$

$$\rho C_P \left(\frac{\partial T}{\partial t} + \mathbf{u} \cdot \nabla T \right) = \nabla \cdot (k \nabla T) + \eta \dot{\gamma}^2 \tag{4}$$

where $\mathbf{u}$ is the velocity vector, T is the temperature, t is the time, p is the pressure, $\boldsymbol{\sigma}$ is the total stress tensor, ρ is the density, η is the viscosity, k is the thermal conductivity, C_p is the specific heat and $\dot{\gamma}$ is the shear rate. The Finite Volume Method (FVM) due to its robustness and efficiency is employed in this study to solve the transient flow field in complex three-dimensional geometry.

During the cooling process, a three-dimensional, cyclic, transient heat conduction problem with convective boundary conditions on the cooling channel and mold component surfaces is involved. The overall heat transfer phenomenon is governed by a three-dimensional Poisson equation.

$$\rho C_P \frac{\partial T}{\partial t} = k \left(\frac{\partial^2 T}{\partial x^2} + \frac{\partial^2 T}{\partial y^2} + \frac{\partial^2 T}{\partial z^2} \right) \tag{5}$$

where x, y, and z are the Cartesian coordinates.

After the ejection, the part experiences a free shrinkage due to the temperature and pressure change. The warpage analysis assumes the mechanical properties are linear-elastic. The stress-strain equations enable us to solve the problems.

$$\boldsymbol{\sigma} = \mathbf{C}\left(\varepsilon - \varepsilon^0 - \alpha \Delta T\right) \qquad (6)$$

$$\varepsilon = \frac{1}{2}\left(\nabla \mathbf{D} + \nabla \mathbf{D}^T\right) \qquad (7)$$

where $\mathbf{C}$ is the 4th tensor related to the material mechanical properties, ε is the strain tensor, α is CLET tensor and $\mathbf{D}$ is the displace tensor.

Model and Related Information

The geometry and dimension of the runners and cavities are shown as in Figure 2. The diameter of each cavity is 60 mm with 3.5 mm thickness. The material applied is GPPS_POLYREXPG-22. The viscosity property of this material is listed in Figure 3. Process conditions are given in Table 1, including filling time, mold temperature, melt temperature, packing time, and so on. Furthermore, to capture the flow behavior of each branch, we assign identity numbers 1, 2, 3 for each runner as shown in Figure 4(a). L_1, L_2, L_3 is labeled accordingly in Figure 4(b) to quantify core material penetration length in runner when one of its branched first reach cavity. As of final penetration length in cavity at end of filling, C_X represents the core penetration length in flow direction, C_Y in perpendicular to core flow direction, C_Z in thickness direction.

Results and Discussion

Figure 6 shows the core penetration shape in black as skin/core=72/28. When the injection speed is low as 10 cm³/sec, the longest core penetration happens in Branch 1 (as shown in L_1). As the injection speed is increased, the core penetration is enhanced in Branch 2 and 3. Until injection speed is up to 16 cm³/sec, the longest core penetration happens in Branch 2 (as shown in L_2). The detailed dynamic variation for the penetration distance for each branch is displayed in Figure 7. The switching speed is around 16 cm³/sec.

Furthermore, it is also very important to see core penetration phenomena at the end of filling for all possible injection conditions. Following the behavior in the runner, core penetration is also different at end of filling with the change of injection speed. Figure 8 shows the final core penetration behavior of each branch. White is skin material, and blue is core material. If a certain cavity is fully filled with skin material (first shot), then core material (second shot) is not able to push further. For low injection speed, cavity 1 still left little space for second shot when it enters at 72% volume filled with first shot. For high injection speed, the first shot material is occupied more in the runner and cavity for Branch 1, and

then the second shot will stopped in the runner. This is because cavity 1 is filled with skin material and leave no room for core material to enter at 72% volume filled. Quantified core material penetration length at the end of filling is shown in Figure 9. Generally speaking, C_X, C_Y, C_Z are longer in low injection speed. It would leave more space in the cavity when second shot start entering. However, during the high injection speed period, more core material is penetrated in the runner system, it is the reason why all three direction penetration in cavity is less.

Moreover, the core penetration distance is also very sensitive to skin/core ratio in co-injection system. We are curious about how this sensitivity is in co-injection multi-cavity system. The original core material entering setting is 72% volume filled with skin material (i.e., skin/core volume ration is 72/28). Figure 10 (a) shows the core material penetration length when one of its branched first reach cavity. Clearly, with core ratio of 28% or higher, the core penetration length of the Branch 1 reaches cavity first. However, when it is switched to lower core ratio (say skin/core=84/16), the core penetration length of Branch 2 and 3 reach cavity first. The dynamic behavior is dramatically changed. Figure 10 (b) shows the core penetration behavior till the end of filling. Obviously, the more core ratio, the longer core penetration runs through runner to cavity. Due to the multi-cavity geometrical structure, the core penetration is unbalance for each cavity.

Finally, the simulation is validated with the literature result [9]. Figure 11 displayed the flow front of the skin layer when flow front of any Branch touches the cavity. We can see that whether in high or low speed condition, Branch 1 always reaches first regardless of change in mold temperature and injection speed. Figure 12 shows the core penetration flow front. For low injection speed (10.2 cm³/sec) L_1 is the longest in runner, and for high injection speed (51 cm³/sec) L_2 takes the lead. These results show both simulation and experiments are in a good agreement in trend. As for middle injection speed (35.7 cm³/sec), simulation shows L_2 is the longest branch while experiment result in L_1 the longest instead. This is because simulation and experiment use similar property materials yet not exactly the same one. Therefore the trend of switching leading branch of core material is caught, but the critical switching injection speed might not be the same for simulation and experiment.

Conclusions

In this study, we have focused on dynamic behavior of core-material penetration in a co-injection multi-cavity molding. The dynamic behavior of core penetration is very sensitive to injection speed and also skin/core ratio. It can be changed dramatically from one runner to the other (from Branch 1 switch to Branch 2 and 3 in our case). In addition, from the results of the core penetration behavior till end of filling, the more core ratio it is, the longer core penetration runs through runner to cavity.

However, due to the multi-cavity geometrical structure, the balance of the core penetration for multi-cavity is still a challenge. Finally, the simulation is validated with the literature result [9]. These results show both simulation and experiments are in a good agreement in trend.

References

1. P.J. Garner and D.F. Oxley, British Patent 1,156,217, 1971.
2. V. Goodship and J.C. Love, Multi-Material Injection Molding, 2002.
3. S.-P. Sun, C.-C. Hsu, C.-T. Huang, K,-C. Huang and S.-C. Tseng, SPE-ANTEC Conferences, 2012
4. Jimmy C.Chien, Chao-Tsai Huang, Wen-Hsien Yang, David C.Hsu, SPE ANTEC 2006
5. Ching-Chang Chien, Yi-Hui Peng, Wen-Li Yang, and Rong-Yeu Chang, "EFFECTS OF MELT ROTATION ON WARPAGE PHENOMENA IN INJECTION MOLDING", SPE ANTEC, 2007
6. John P. Beaumont / Beaumont Runner Technologies, Inc. "Intra-Cavity Filling Imbalances" Technical Brief 2001,10
7. John P. Beaumont and Jack H. Young, "Mold Filling Imbalances in Geometrically Balanced Runner Systems" Journal of Injection Molding Technology, September 1997, Vol. 1, No. 3
8. John P. Beaumont, "Runner and Gating Design HandBook".
9. W.M. Yang, H. Yokoi, Polymer Testing, 22, 37, 2003.
10. Web source: http://commons.wikimedia.org/wiki/File:Co-injection_(sandwich)_molded_part.jpg , Accessed: Nov. 25, 2014.
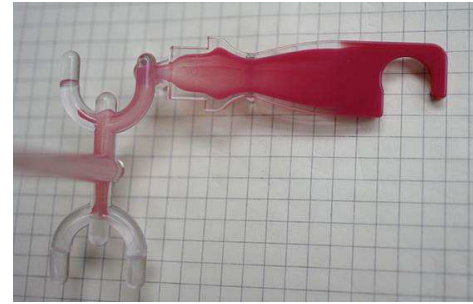
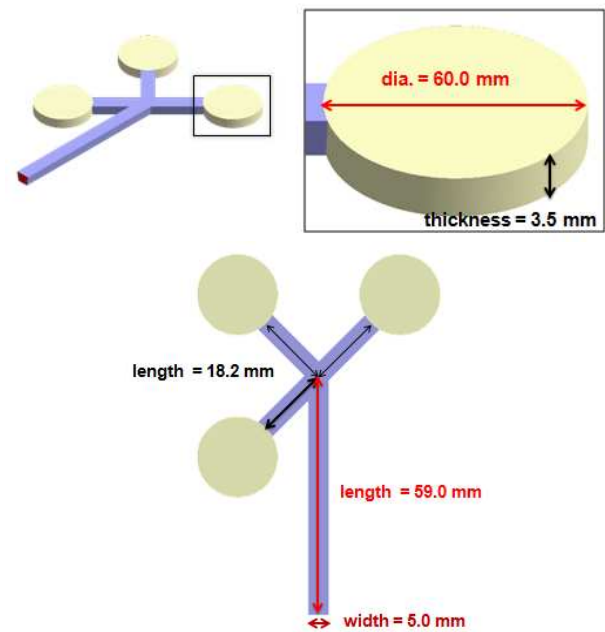Figure 1: An example of co-injection molding with fork structure [10].

Figure 2. Geometry model and dimension

Table 1. Process condition for simulation

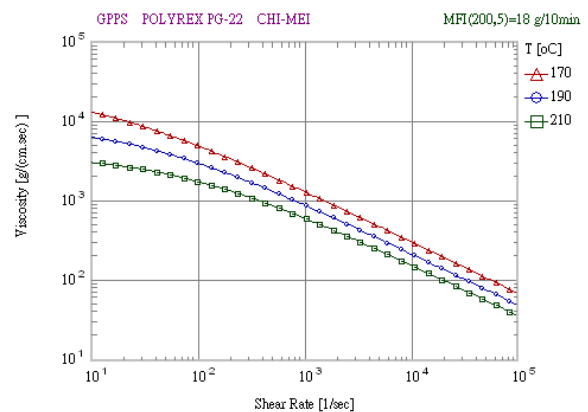|	
Filling Time	0.60 (sec)
Melt Temperature	220.0 (°C)
Mold Temperature	60.0 (°C)
Maximum Injection Pressure	250.0 (MPa)
Material	GPPS POLYREX PG-22
Packing Time	0.05 (sec)
Maximum Packing Pressure	250.0 (MPa)
Mold Opening Time	5.0 (sec)
Ejection temperature	97.0 (°C)
Air Temperature	25.0 (°C)
Core enter Time (by volume filled)	72 (%)

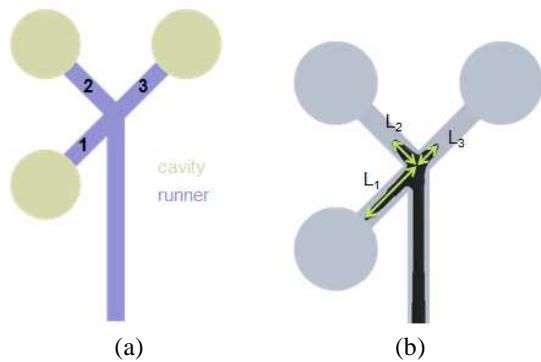Figure 3. Viscosity/shear rate diagram for simulation materials

Figure 4. (a) the identity number for runner, (b) capture core material penetration length when one of its branched first reach cavity, L_1 for branch 1, and so on.
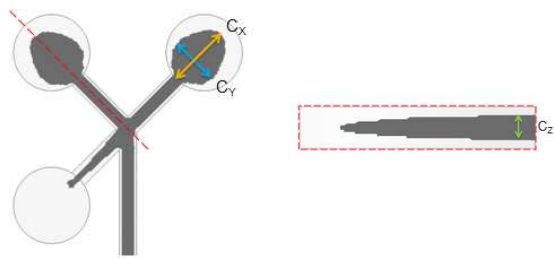

Figure 7. The transition for the core material penetration length switch from L_1 to L_2 at various injection speeds.

Figure 5. Capture core material penetration length at the end of filling: C_X in flow direction, C_Y in perpendicular to flow direction, C_Z in thickness direction.
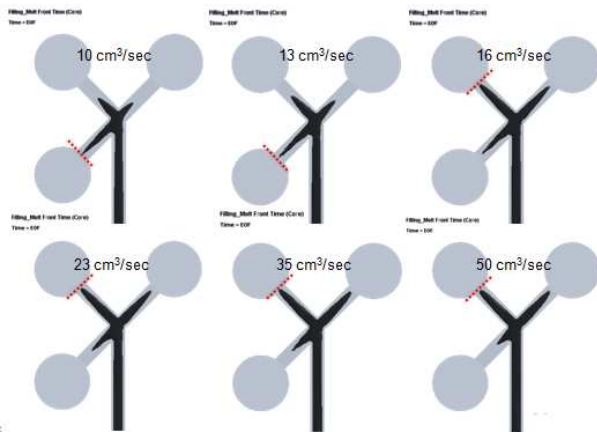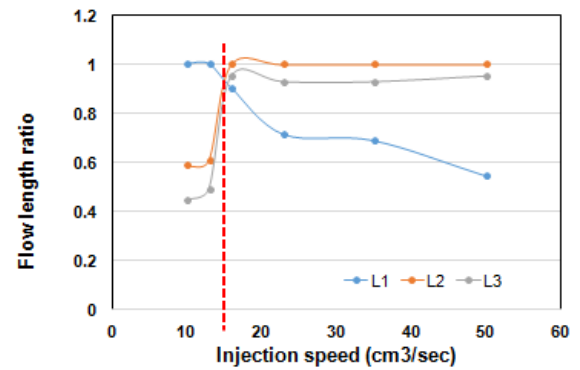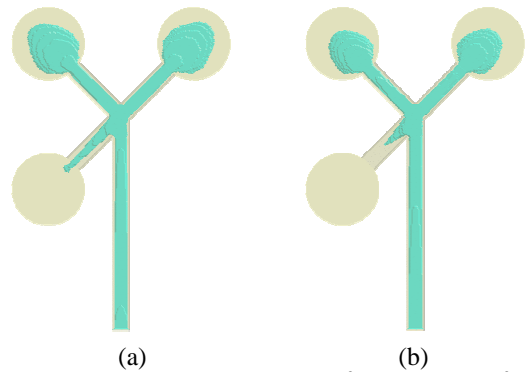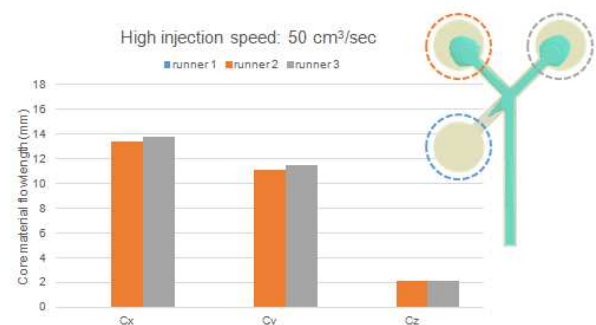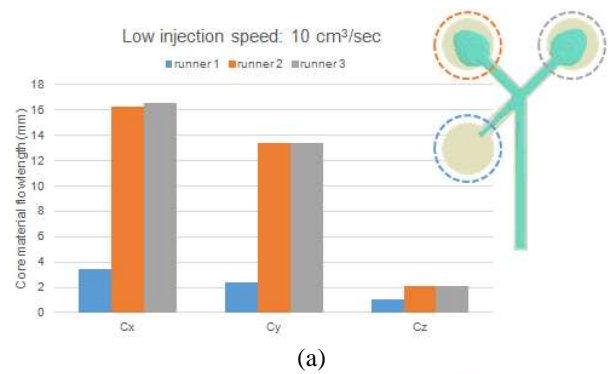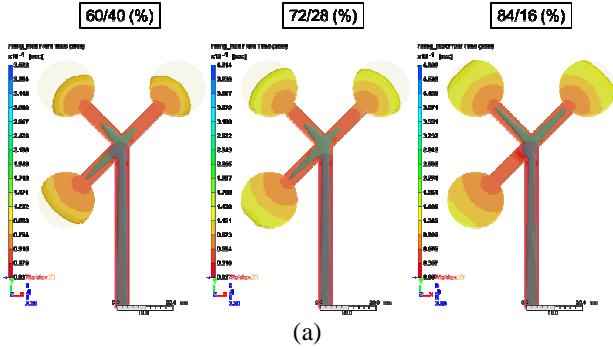

(a)   (b)

Figure 8. (a) injection speed = 10cm^3/sec (b) 50 cm^3/sec; Core penetration location differ because of different injection speed

Figure 6. Core material penetration length switch from L_1 to L_2 at 16 cm^3/sec. Skin/core= 72/28.
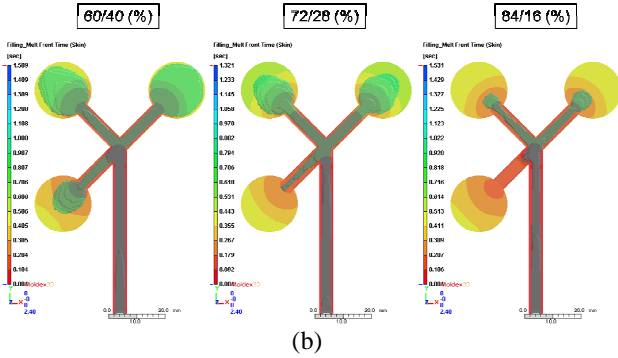
(b)

Figure 9. Core penetration in three directions as C_X, C_Y, and C_Z under different injection speed: (a) 10 cm^3/sec, (b) 50 cm^3/sec.
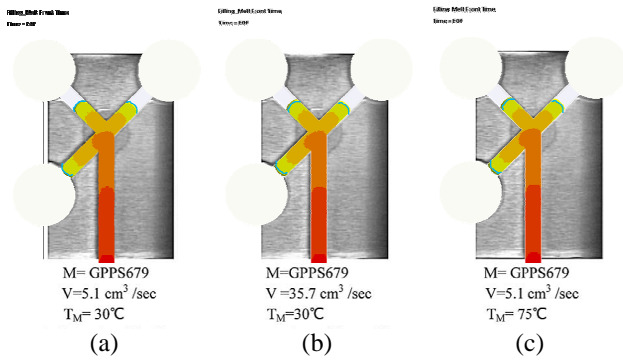

(a)

(b)

Figure 10. Melt front under different skin / core material volume ratio (a) capture core material penetration length when one of its branched first reach cavity, (b) at EOF
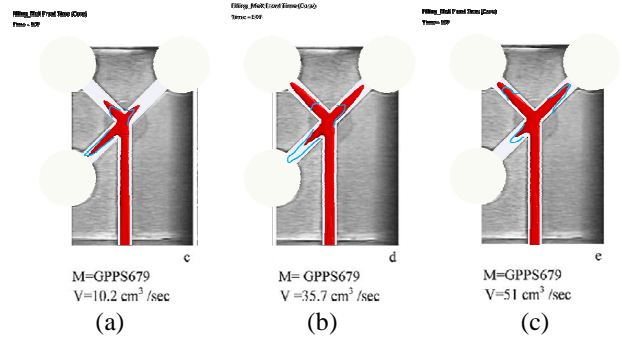

M= GPPS679 V=5.1 cm^3 /sec T$_M$= 30℃	M=GPPS679 V =35.7 cm^3 /sec T$_M$=30℃	M= GPPS679 V=5.1 cm^3 /sec T$_M$= 75℃
(a)	(b)	(c)

Figure 11. Experiment validation (skin layer). Blue line is experiment melt front, colored red/orange/yellow area is simulation melt front of skin material.

M=GPPS679 V=10.2 cm^3 /sec	M= GPPS679 V =35.7 cm^3 /sec	M=GPPS679 V=51 cm^3 /sec
(a)	(b)	(c)

Figure 12. Experiment validation (core layer). Blue line is experiment melt front, colored red area is simulation melt front of core material.